



The Archean sedimentary sulfur recycling under the Kaapvaal craton revisited from 4S-isotopic compositions in sulfide inclusions in diamonds from Kimberley Pool (South Africa) Jwaneng and Orapa (Botswana)

E Thomassot^{1,2}, J Farquhar³, N Bouden¹, J.W Harris⁴, K. McKeegan⁵, J Cliff⁶
B Wing⁷, P Piccoli³

¹ CRPG-CNRS and Université de Lorraine, 54501 Vandœuvre-Lès-Nancy, France

² Institut de Physique du Globe de Paris, 1 Rue Jussieu, 75 005 Paris, France.

³ University of Maryland, Washington, United States.

⁴ University of Glasgow, Glasgow, Scotland, UK.

⁵ UCLA, Los Angeles, United States.

⁶ Pacific Northwest National Lab, Richland, United States.

⁷ University of Colorado, Boulder, United States.

Introduction

The sulfur isotope composition of sulfide inclusions in diamond (SID) provides evidence for recycling of sulfur in the diamond stability field. Variations of $\delta^{34}\text{S}$ (Chaussidon 1987; Rudnick 1993) and mass-independent fractionation (S-MIF, Farquhar 2002; Thomassot 2009) are not readily explained by mantle processes and are better attributed to recycling of sulfur with surface $\delta^{34}\text{S}$ and S-MIF signatures. Variations of $\delta^{34}\text{S}$ are large in sedimentary rocks principally because of the role played by microbially-mediated sulfur metabolisms. On the other hand, S-MIF signatures result from photochemical reactions involving ultra-violet (UV) light and were produced in the atmosphere before the Great Oxygenation Event (GOE). Consequently, the presence of S-MIF is diagnostic of Archæan sedimentary sulfur and as such, is one of the most robust geochemical tools for tracking the possible recycling of Archæan surficial sulfur transported to deep-seated rocks.

In sediments, the relative abundance of the minor isotope of sulfur, ^{36}S , is also affected by both mass-dependent reactions (related to microbial cycling, e.g. Ono et al., 2006) and mass-independent atmospheric reactions that lead to variations of $\delta^{34}\text{S}$ and $\Delta^{33}\text{S}$. Accordingly, studying covariations of $\Delta^{33}\text{S}$ and $\Delta^{36}\text{S}$ helps in deciphering peculiar fractionation processes.

Here we use the 4S-isotope signatures in SID *i)* to test the robustness of S-MIF array of specific exospheric sulfur pools along their journey from the surface to the mantle and *ii)* to provide a more complete assessment of the recycled sulfur pools and map the sedimentary ingredients recycled from the surface to the diamond growth-environment.

Samples and Methods

We have selected 40 SID originating from three distinct kimberlite pipes (Jwaneng and Orapa in Botswana, and Kimberley Pool in South Africa) located along the Colesberg Lineament (Kaapvaal craton). This N-S magnetic anomaly represents the suture zone between the eastern and western blocks of the craton, and the cratonic keels below this area likely preserve subducted surficial lithologies as attested by the large proportion of eclogitic xenoliths carried to the surface by kimberlites (Shirey et al., 2003). Among the entire collection, three samples have a peridotitic affinity whereas the other are clearly eclogitic. Samples from Orapa (n=18) and Jwaneng (n= 18) have been analyzed earlier for $\delta^{34}\text{S}$ and $\Delta^{33}\text{S}$ (Farquhar et al., 2002; Thomassot et al., 2009).

We examine the $\Delta^{36}\text{S}$ in addition to $\delta^{34}\text{S}$ and $\Delta^{33}\text{S}$ signatures measured in-situ with secondary ion mass spectrometers (CAMECA 1280 at UCLA and UWA and 1280 HR at CRPG Nancy). The same measurement protocol (Cs^+ primary source, multicollection mode with 3 faraday cups and one electron multiplier for ^{36}S) has been used in all three laboratories. However, instrumental fractionation

correction differs from one laboratory to the other (Laflamme et al., 2017 for UWA and Delavault et al., 2016 for CRPG). Results of the interlaboratory measurement comparison are in good agreement and will be presented at the conference. Two sigma external uncertainties are better than ± 0.15 ‰ for single $\Delta^{33}\text{S}$ measurements and ± 0.35 ‰ for single $\Delta^{36}\text{S}$ measurement.

Results

The sulfur isotopic composition in SID from Jwaneng ($\delta^{34}\text{S}$ from -6.7 ‰ to 3.14 ‰, $\delta^{34}\text{S}_{\text{mean}} = -1.04$ ‰), Kimberley Pool ($\delta^{34}\text{S}$ from -8.9 ‰ to 1.9 ‰, $\delta^{34}\text{S}_{\text{mean}} = -1.07$ ‰) displays a wide range centered around the canonical mantle value ($\delta^{34}\text{S} = -1 \pm 2$ ‰, Labidi et al., 2014) whereas Orapa samples are statistically enriched in ^{34}S ($\delta^{34}\text{S}$ from -8.4 ‰ to 1.7 ‰, $\delta^{34}\text{S}_{\text{mean}} = 0.3$ ‰).

Significant mass-independent sulfur isotopic fractionations have been detected in the three localities with differences in amplitude and $\Delta^{36}\text{S}/\Delta^{33}\text{S}$ (Fig. 1). In Jwaneng samples, significant and (mostly) positive $\Delta^{33}\text{S}$ (ranging from -0.25 to 1.65 ‰) associated with negative $\Delta^{36}\text{S}$ (ranging from -1.67 to 0.29 ‰) match a global negative trend ($\Delta^{36}\text{S}/\Delta^{33}\text{S} = -1.1 \pm 0.23$). In Kimberley Pool, these anomalies are smaller with negative $\Delta^{33}\text{S}$ (from -0.28 to -0.04 ‰) and negative $\Delta^{36}\text{S}$ from $(-1.4$ to -0.3 ‰), defining a weak positive correlation ($\Delta^{36}\text{S}/\Delta^{33}\text{S} = +0.8$). Finally, five samples from Orapa possess positive $\Delta^{33}\text{S}$ (up to 1.3 ‰). The remaining Orapa samples, which are devoid of large $\Delta^{33}\text{S}$ anomalies, are interestingly enriched in ^{36}S (i.e. $\Delta^{36}\text{S}$ ranging from 0 to 1 ‰) and define a trend such as $\Delta^{36}\text{S}/\Delta^{33}\text{S} = -8$.

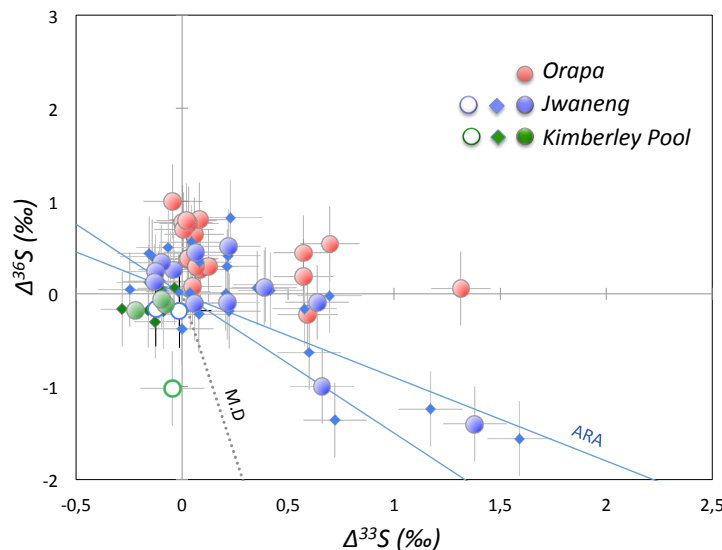


Figure 1 :

Plot of $\Delta^{36}\text{S}$ versus $\Delta^{33}\text{S}$ values determined in situ for sulfides inclusions in diamonds from Jwaneng (blue symbols), Kimberley Pool (green symbols) and Orapa (red symbols).

Plain symbols: E-type specimens

Open symbols: P-type specimens

Diamonds symbols refer to individual measurements. Dot symbols refer to averaged values for a single inclusion.

The blue lines represent the array found in most of Archean sediments ($\Delta^{36}\text{S}/\Delta^{33}\text{S}$ ranging from -0.9 to -1.5). The dotted line represents the mass-dependent fractionation ($\Delta^{36}\text{S}/\Delta^{33}\text{S} = -7$)

Discussion

Re/Os studies in SID originating from the Kaapvaal craton revealed two main groups of ages. A large number of inclusions from the Jwaneng, Kimberley Pool and Orapa plot on a 2.9 Ga isochron with the remainder displaying weaker isochron ages ranging from 1.9 to 1 Ga (Richardson 2001; Shirey et al. 2008). Comparing our results with the isotopic record in sediments from comparable ages, reveals some similarities.

The general isotopic trend found in Jwaneng SID matches the ARA (Fig 2a) and provides a robust confirmation of the recycling of neo-Archean sediments (Thomassot et al., 2009).

Multiple S-isotopic signatures in Kimberley Pool samples clearly differ from Jwaneng implying a distinct source of sulfur. S-MIF covariations in this location are more elusive as the amplitude of both $\Delta^{33}\text{S}$ and $\Delta^{36}\text{S}$ are small. However Kimberley Pool SID match the composition of some meso-Archean sediments (Fig 2b), in good agreement with the meso-Archean isochron age reported in the literature.

Finally, Orapa samples can be divided into two subpopulations. A small group of samples is consistent with an Archean S-MIF signature comparable with Jwaneng samples. The remaining samples, without clearly anomalous $\Delta^{33}\text{S}$ and $\delta^{34}\text{S}$, carry significant variations for $\Delta^{36}\text{S}$ which are

consistent with isotopic fractionation accompanying microbial sulfate reduction (Ono et al., 2006). It is worth noting that the S-MIF trend in Orapa matches the composition of sedimentary sulfur deposited at the surface of the Earth 1.9 ± 0.2 Ga corresponding to one Re/Os isochron age determined for this locality (Shirey et al., 2008).

This study confirms that surficial sulfur has been efficiently transferred to the lithospheric mantle. More interestingly, it shows that S-MIF isotopic signatures (i.e. $\Delta^{36}\text{S}/\Delta^{33}\text{S}$) are preserved during the recycling of sediment. Complementary to radiogenic isotope data, 4S- isotope measurements are thus robust probes for spotting different sedimentary pools (e.g. deposited at different periods of time, or corresponding to different environmental conditions) in mantle rocks.

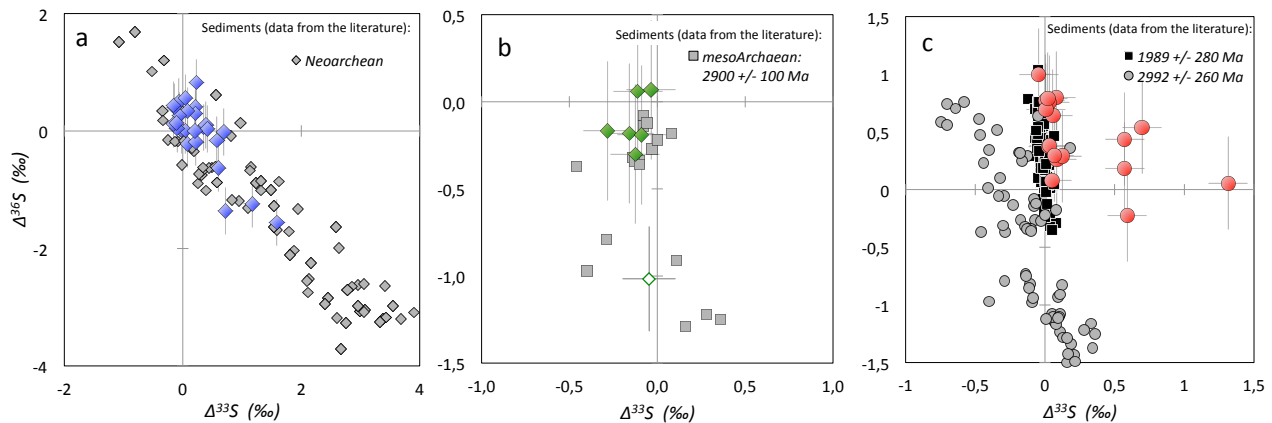


Figure 2 : Plots of $\Delta^{36}\text{S}$ versus $\Delta^{33}\text{S}$ values measured in SID from a) Jwaneng, b) Kimberley Pool and c) Orapa (see Fig 1 for symbol description). The grey symbols are shown for comparison and represent multiple sulfur isotope compositions in sediments from different period of time (data from the literature).

References:

- Chaussidon M., et al. (1987). Sulphur isotope heterogeneity in the mantle from ion microprobe measurements of sulphide inclusions in diamonds. *Nature*, 330(6145), 242-244.
- Delavault, H. et al. (2016). Sulfur and lead isotopic evidence of relic Archean sediments in the Pitcairn mantle plume. *Proceedings of the National Academy of Sciences*, 113(46), 12952-12956.
- Farquhar, J., Bao, H., & Thiemens, M. (2000). Atmospheric influence of Earth's earliest sulfur cycle. *Science*, 289(5480), 756-758.
- Farquhar, J. et al. (2002). Mass-independent sulfur of inclusions in diamond and sulfur recycling on early Earth. *Science*, 298(5602), 2369-2372.
- Izon, G. et al. (2017). Biological regulation of atmospheric chemistry en route to planetary oxygenation. *Proceedings of the National Academy of Sciences*, 114(13), E2571-E2579.
- Ono, S., et al. (2006). Mass-dependent fractionation of quadruple stable sulfur isotope system as a new tracer of sulfur biogeochemical cycles. *Geochimica et Cosmochimica Acta*, 70(9), 2238-2252.
- Labidi, J. et al. (2014). Sulfur isotope budget (^{32}S , ^{33}S , ^{34}S and ^{36}S) in Pacific-Antarctic ridge basalts: A record of mantle source heterogeneity and hydrothermal sulfide assimilation. *Geochimica et Cosmochimica Acta*, 133, 47-67.
- LaFlamme, C. et al. (2016). In situ multiple sulfur isotope analysis by SIMS of pyrite, chalcopyrite, pyrrhotite, and pentlandite to refine magmatic ore genetic models. *Chemical Geology*, 444, 1-15.
- Rudnick, R. L. et al. (1993). Diamond growth history from in situ measurement of Pb and S isotopic compositions of sulfide inclusions. *Geology*, 21(1), 13-16.
- Shirey, S. B., et al. (2008). A review of the isotopic and trace element evidence for mantle and crustal processes in the Hadean and Archean: Implications for the onset of plate tectonic subduction. *Geological Society of America Special Papers*, 440, 1-29.
- Thomassot, E., et al. (2009). Metasomatic diamond growth: A multi-isotope study (^{13}C , ^{15}N , ^{33}S , ^{34}S) of sulphide inclusions and their host diamonds from Jwaneng (Botswana). *Earth and Planetary Science Letters*, 282(1), 79-90.
- Thomassot, E., et al. (2015). Atmospheric record in the Hadean Eon from multiple sulfur isotope measurements in Nuvvuagittuq Greenstone Belt (Nunavik, Quebec). *Proceedings of the National Academy of Sciences*, 112(3), 707-712.

